JOURNAL OF VIROLOGY, Sept. 2008, p. 8537–8547 Vol. 82, No. 17
0022-538X/08/$08.00+0 doi:10.1128/JVI.00690-08

Small-Molecule Inhibitor Which Reactivates p53 in Human T-Cell Leukemia Virus Type 1-Transformed Cells▽

Kyung-Jin Jung,[1] Arindam Dasgupta,[1] Keven Huang,[1] Soo-Jin Jeong,[1] Cynthia Pise-Masison,[1] Katerina V. Gurova,[2] and John N. Brady[1]*

Virus Tumor Biology Section, Laboratory of Cellular Oncology, Center for Cancer Research, National Cancer Institute, National Institutes of Health, Bethesda, Maryland 20892,[1] and Anti-Cancer Drug Discovery Lab, Cleveland Biolabs, Inc., Buffalo, New York 14203[2]

Received 27 March 2008/Accepted 4 June 2008

Human T-cell leukemia virus type 1 (HTLV-1) is the etiologic agent of the aggressive and fatal disease adult T-cell leukemia. Previous studies have demonstrated that the HTLV-1-encoded Tax protein inhibits the function of tumor suppressor p53 through a Tax-induced NF-κB pathway. Given these attributes, we were interested in the activity of small-molecule inhibitor 9-aminoacridine (9AA), an anticancer drug that targets two important stress response pathways, NF-κB and p53. In the present study, we have examined the effects of 9AA on HTLV-1-transformed cells. Treatment of HTLV-1-transformed cells with 9AA resulted in a dramatic decrease in cell viability. Consistent with these results, we observed an increase in the percentage of cells in sub-G_1 and an increase in the number of cells positive by terminal deoxynucleotidyltransferase-mediated dUTP-biotin nick end labeling assay following treatment of HTLV-1-transformed cells with 9AA. In each assay, HTLV-1-transformed cells C8166, Hut102, and MT2 were more sensitive to treatment with 9AA than control CEM and peripheral blood mononuclear cells. Analyzing p53 function, we demonstrate that treatment of HTLV-1-transformed cells with 9AA resulted in an increase in p53 protein and activation of p53 transcription activity. Of significance, 9AA-induced cell death could be blocked by introduction of a p53 small interfering RNA, linking p53 activity and cell death. These results suggest that Tax-repressed p53 function in HTLV-1-transformed cells is "druggable" and can be restored by treatment with 9AA. The fact that 9AA induces p53 and inhibits NF-κB suggests a promising strategy for the treatment of HTLV-1-transformed cells.

Adult T-cell leukemia (ATL) and human T-cell leukemia virus type 1 (HTLV-1)-related myelopathy/tropical spastic paraparesis are associated with HTLV-1 infection (33). ATL has a low incidence rate and a long latency before onset, suggesting that leukemogenesis is a multistep process (2, 3, 26). The HTLV-1 Tax protein has been shown to play a key role in cellular transformation. Ratner et al., using an infectious molecular clone of HTLV-1, have shown that Tax plays an essential role in lymphocyte immortalization (38). Consistent with these findings, a fragment of the HTLV-1 provirus containing the coding region for Tax was shown to immortalize lymphocytes when cloned into a transformation-defective (44), replication-competent herpesvirus saimiri vector (8). Moreover, studies have shown that Tax expression is sufficient to induce leukemia and neurofibromas in transgenic mice (22), immortalize rat embryo fibroblasts (21), and cooperate with Ras in cellular transformation (36, 44). Further, Akagi et al. have reported that Tax induction can immortalize primary T cells in vitro (1). Models using transgenic animals to examine the in vivo function of Tax further support the key role of Tax in oncogenesis. In these studies Tax expression is sufficient to induce neurofibromas (12), mesenchymal tumors (25), large granular lymphocytic leukemia (9), and pre-T-cell leukemia (11). In addition, transgenic mice expressing Tax under the control of the Lck promoter developed thymus-derived immature T-cell leukemia with characteristics resembling ATL (11).

At least a portion of Tax's transforming activity comes from its function as a transcription transactivator (15, 20, 32). Tax not only transactivates the viral long terminal repeat but also transactivates or transrepresses the expression or function of a wide number of cellular genes, including cytokines, cellular receptors, cell cycle regulators, DNA repair proteins, or proteins that regulate apoptosis (4, 49). For example, the viral transactivator Tax mediates cell cycle progression by targeting key regulators of the cell cycle such as p21/waf1, p53, and cyclin D/cyclin-dependent kinase complexes, thereby deregulating cellular DNA damage and checkpoint control (7).

One protein which is functionally inhibited by Tax is the tumor suppressor p53. p53 controls genetic stability and reduces the risk of cancer through induction of growth arrest and/or apoptosis in response to DNA damage or deregulation of proto-oncogenes (37). p53 is able to induce the expression of genes including Mdm2, p21, BAX, PUMA, and NOXA, which contain p53-binding sites in the promoter regions (46). p53-induced apoptosis is one of the major functions of p53 that is selected against during tumor development. In fact, mutated p53 is observed in about 60% of human cancers. In the majority of HTLV-1-infected cells, p53 is wild type but functionally inactive (34, 35).

Constitutively active NF-κB contributes to inhibiting apoptosis and promoting proliferation by stimulating expression of antiapoptotic factors and cytokines (28). Although a direct interaction between Tax and different members of the NF-κB

* Corresponding author. Mailing address: Virus Tumor Biology Section, Laboratory of Cellular Oncology, Center for Cancer Research, National Cancer Institute, Building 41, Room B201, National Institutes of Health, Bethesda, MD 20892. Phone: (301) 496-0986. Fax: (301) 496-4951. E-mail: bradyj@exchange.nih.gov.

▽ Published ahead of print on 11 June 2008.

family has been reported, the primary action of Tax in activating NF-κB appears to occur through interaction with IκB kinase γ (IKKγ) in the IKK signalosome, which includes IKKα, IKKβ, NF-κB-inducing kinase, and MEKK1 (mitogen-activated protein kinase/extracellular signal-regulated kinase kinase kinase 1). A more comprehensive discussion of this topic can be found in reviews on Tax activation of NF-κB (13, 14). Recent studies showed that AKT is also a signaling intermediate upstream of NF-κB-dependent survival gene expression. AKT can promote the activation of NF-κB by phosphorylation of IKK, resulting in IκBα phosphorylation and degradation (6, 30, 39) and augmenting the transcription activity of NF-κB p65/RelA (24, 30). Also, AKT and IKKα/β have been reported to be direct activating kinases that phosphorylate Ser536 of p65 (19, 23, 27, 40, 41). Recent studies have shown that Tax mediates activation of AKT by mediating phosphorylation at Ser473 and Thr308 (16, 17) and that the role of Tax-activated AKT in cell proliferation is through direct interaction with the p85 subunit of phosphatidylinositol-3 kinase (31).

Recent studies from this laboratory have demonstrated a strong link between Tax's ability to activate NF-κB and its ability to inhibit p53 in lymphocytes (34). Of interest, blocking NF-κB activation by expressing a dominant negative IκBα protein or by inhibiting the NF-κB pathway using the IKKβ-specific inhibitor SC514 has been shown to block Tax-mediated p53 inhibition in Tax-transfected and HTLV-1-transformed cells (18, 34). In both cases the inhibitory effects of Tax and NF-κB were neutralized, and transcription activity of the wild-type p53 was reactivated. The fact that p53 can be reactivated in HTLV-1-transformed cells indicates it is "druggable" and offers an ideal target for the development of specific ATL-targeted drugs.

Similar to ATL cells, renal cell carcinoma (RCC) cells contain wild-type p53, which is repressed by constitutively active NF-κB (10, 29). The ability of 9-aminoacridine (9AA) to simultaneously inhibit NF-κB and reactivate p53 in RCC cells made it an attractive small-molecule inhibitor to examine in ATL cells. In this report, we demonstrate that treatment of HTLV-1-transformed cells with 9AA causes a significant decrease in cell viability. We provide further evidence that 9AA inhibits NF-κB and reactivates p53 in HTLV-1-transformed cells. That p53 reactivation is linked to cell death is demonstrated by the fact that a p53 small interfering RNA (siRNA) inhibits 9AA-induced cell death. These finding suggest that p53 in ATL cells might serve as a molecular target for therapeutic intervention.

MATERIALS AND METHODS

Preparation of PBMCs. Heparinized human peripheral blood was obtained from healthy volunteers from the NIH clinical center. Peripheral blood mononuclear cells (PBMCs) were isolated with the Ficoll-Paque Plus (GE Healthcare) by the gradient density method as described in the manufacturer's instructions. The PBMCs were stimulated with the mitogen phytohemagglutinin-P in the presence of human interleukin-2 (IL-2) for 24 h before use.

Cell culture and drug treatment. HTLV-1-transformed cell lines C8166, MT-2, and Hut102 and T-lymphocyte cell line CEM were maintained in RPMI medium supplemented with 10% fetal calf serum, 2 mM L-glutamine, and penicillin/streptomycin. PBMCs, SP cells, and ATL15 cells were cultured with IL-2 in 20% fetal bovine serum-enriched RPMI medium with IL-2 before drug treatment. For treatment with 9AA, 5×10^5 to 7×10^5 cells/ml were cultured in medium in 100-mm^2 dishes or T75 culture flasks.

Plasmids, transfection, and luciferase assay. The reporter constructs PG13-Luc and 4×NF-κB-Luc have been described previously (34, 35). For luciferase assays, cell lysates were prepared 24 h after transfection with TransFast (Promega), and activity was measured with a dual luciferase assay system (Promega) and GalactoLight assay kit (Tropix) per the manufacturer's instructions. All transfections included the control plasmid cytomegalovirus (CMV)-β-galactosidase to control for transfection efficiency.

Cell viability. Cell viability assays were performed using two different assays. First, to quantitate ATP generated by metabolically active cells, assays were performed using a CellTiter-Glo luminescent cell viability assay (Promega) per the manufacturer's instruction. Briefly, 5×10^5 to 7×10^5 cells/ml were cultured in sterile 96-well plates in the presence of increasing concentrations of 9AA (0 to 20 μM) in RPMI medium. The plates were then incubated for 24 to 48 h, and then 100 μl of CellTiter-Glo reagent was added to lyse the cells. After a 10-min incubation at room temperature, the luminescence was recorded in a luminometer with an integration time of 1 s per well. The luminescence signals for the 9AA-treated cells were normalized by the luminescence signal obtained from dimethyl sulfoxide (DMSO)-treated cells. As an alternative method to quantitate cell viability, the trypan blue exclusion dye method was used. DMSO- or 9AA-treated cells were assayed by adding trypan blue solution (0.4% in phosphate-buffered saline [PBS]) to the culture medium. After 3 min, the number of dead cells that retained the dye was compared to the total number of cells to calculate cell viability.

Cell cycle analysis. Cells were harvested and fixed in cold 70% ethanol and incubated overnight at 4°C. Fixed cells were then resuspended in 100 μl and stained with propidium iodide (PI) (50 μg/ml) after treatment with 100 μl of RNase (10 mg/ml). The stained cells were analyzed for DNA content using a FACSCalibur instrument (Becton Dickinson Bioscience). Cell cycle fractions were quantified with Cell Quest (Becton Dickinson Bioscience) and analyzed by ModFit or FlowJo software.

TUNEL assay. To quantitate apoptosis, a terminal deoxynucleotidyltransferase (TdT)-mediated dUTP biotin nick end labeling (TUNEL) assay was done with an APO-bromodeoxyuridine (BrdU) TUNEL assay kit (Molecular Probes) following the manufacturer's instructions. Briefly, C8166 cells (10^6 cells) were fixed with 1% paraformaldehyde (Pierce) in 1× PBS, followed by treatment with 75% ethanol for 16 to 18 h at 4°C. The fixed cells were incubated with TdT at 37°C (Molecular Probes), stained with Alexa Fluor 488 dye-conjugated anti-BrdU monoclonal antibody for 30 min at room temperature away from light, and then treated with PI-RNase A staining buffer for 30 min at room temperature. The immunostained cells were then analyzed using a FACSCalibur (Becton Dickinson Bioscience). TUNEL-positive cells were quantified with Cell Quest and FlowJo software.

Western blot analysis. Cell extracts were prepared by using radioimmunoprecipitation assay lysis buffer supplemented with protease inhibitor cocktail (Roche) and phosphatase inhibitor cocktail (Sigma). Cells were resuspended in lysis buffer and incubated on ice for 15 min. After a thorough vortexing, the samples were centrifuged at 14,000 rpm, and supernatants were collected for analysis. For the nuclear extracts, cells were lysed with NE-PER nuclear and cytoplasmic extraction reagents (Pierce). A total of 50 to 100 μg of protein sample was separated by sodium dodecyl sulfate-polyacrylamide gel electrophoresis and transferred to Immobilon-P membranes (Millipore). The membranes were blocked with PBS containing 0.1% Tween and 5% bovine serum albumin and then probed with the appropriate antibody. Chemiluminescence was detected by enhanced chemiluminescence reagent (GE Healthcare).

Reverse transcription-PCR (RT-PCR). Total RNA was prepared with Trizol reagent (Invitrogen) using the manufacturer's protocol. One microgram of total cellular RNA was reverse transcribed with oligo(dT) using the ImPromII reverse transcription kit (Promega) in a 20-μl reaction volume. Primer sequences used in the study were as follows: 6-carboxyflorescin-labeled Mdm2 and glyceraldehyde-3-phosphate dehydrogenase (GAPDH) primers were purchased as 20× stocks from Applied Biosystems. The PCRs contained 1× Sybr Green mix (Stratagene), a 400 nM concentration of each primer, and 50 ng of cDNAs. Fivefold dilutions of the cDNA pool from the "untreated control" were run to generate standard curves. The values of the PCR products were normalized to the values obtained with β-actin mRNAs. Standard curves generated from the control mRNA were used to determine the relative change in the mRNA values.

EMSA. Electrophoretic mobility shift assay (EMSA) was used to characterize the binding activity of NF-κB in nuclear extracts. The sequence used for wild-type NF-κB binding sites was 5′-AGTTGAGGGGACTTTCCCAGGC-3′, while the mutant NF-κB oligonucleotide was 5′-AGTTGAGGCGACTTTCCCAGGC-3′. Complementary oligonucleotides were annealed to create the double-stranded DNA probe. Each strand was labeled with biotin-11-dUTP (Pierce). Gel shift assays were performed with 15 to 25 μg of nuclear extract in the

presence of 1 μg of poly(dI-dC)-poly(dI-dC). Samples were incubated at room temperature for 20 min and loaded onto a 5% native polyacrylamide gel in a running buffer of 0.5× Tris-borate-EDTA buffer. Following electrophoresis, the gel was transferred to a Biodyne B membrane (Pierce), and bands were detected by streptavidin-horseradish peroxidase chemiluminescent substrate.

Adenovirus infection of cells. The adenovirus green fluorescent protein (adeno-GFP) and p53 siRNA (adeno-p53 siRNA) constructs were kindly provided by Ling-Jun Zhao (St. Louis University). The recombinant viral genome was linearized and transfected into 293 cells. Eight days after transfection, the recombinant virus was collected and subjected to one round of amplification by infecting 1.5×10^6 293 cells, yielding 2 ml of viral stocks. For infection of HTLV-1-transformed C8166 cells (1.5×10^6), adeno-p53 siRNA or adeno-GFP was incubated with cells in serum-free RPMI medium. After 3 h, cells were washed and resuspended in RPMI medium containing 10% fetal bovine serum. The infected cells were incubated for 48 h for adenovirus expression and then treated with either DMSO or 9AA for 48 h.

Proliferation assays. Cell proliferation was measured with a nonradioactive cell proliferation assay (Promega), which is a colorimetric method for determining proliferation by using 3-(4,5-dimethylthiazol-2-yl)-5-(3-carboxymethoxyphenyl)-2-(4-sulfophenyl)-2H-tetrazolium (MTS) and phenazine methosulfate (PMS). Briefly, cells were seeded in a 96-well assay plate containing 100 μl of 50,000 cells/well and treated with 9AA for 24 to 72 h. At the end of incubation time, the combined MTS/PMS solution was added into each well and incubated for 3 h at 37°C. Then, 25 μl of 10% sodium dodecyl sulfate was added to each well to stop the reaction for 30 min, and the absorbance measured at 490 nm with an enzyme-linked immunosorbent assay plate reader.

RESULTS

9AA decreases cell viability of HTLV-1-transformed cells. We first analyzed the effect of 9AA on HTLV-1-transformed cell viability. HTLV-1-transformed cell lines C8166, Hut102, and MT2 were compared to control PBMCs and CEM lymphocytes. HTLV-1-transformed cells and control cells were treated with 20 μM 9AA for 48 h. At the end of the incubation period, cells were harvested, and cell viability was measured by a CellTiter-Glo luminescent cell viability kit (Promega) which quantitates the ATP generated in viable cells. The results presented in Fig. 1A demonstrate that the HTLV-1-transformed cell lines were more sensitive to treatment with 9AA than PBMCs and CEM cells. At 48 h, approximately 90% cell death was observed in both the C8166 and MT2 cell cultures. Hut102 cells were slightly more sensitive, with 95% cell death observed. In contrast, the control PBMCs and CEM cells were less sensitive to 9AA, with CEM cells showing only 40% cell death at 48 h.

We also analyzed cell viability by the trypan blue exclusion assay. Similar to the results obtained with the CellTiter-Glo luminescent cell assay, the HTLV-1-transformed cells were more sensitive than controls to treatment with 9AA (Fig. 1B). While 85 to 90% cell death was observed with the HTLV-1-transformed cells, approximately 50% cell death was observed in the control PBMC and CEM cultures.

We next analyzed the effect of 9AA on cell proliferation. In the initial experiment, the concentration of 9AA was titrated, and cell proliferation was measured at 48 h posttreatment. The results presented in Fig. 1C demonstrate that while 9AA inhibits proliferation of all cells tested, it displays preferential inhibition of HTLV-1-transformed cell growth. At the highest concentration of 9AA tested (20 μM), proliferation of uninfected transformed CEM cells was inhibited by 30% while the proliferation of HTLV-1-transformed C8166, SP, and MT2 cells was inhibited approximately 60%. Of interest, proliferation of leukemic cells from an ATL patient was inhibited by greater that 95% at 20 μM 9AA. The data presented in Fig. 1D represent time course proliferation assays at two concentrations of 9AA, 10 and 20 μM. The results of these assays, consistent with the data presented in Fig. 1C, show that 9AA preferentially inhibits proliferation of HTLV-1-transformed cells.

FACS and TUNEL analysis of 9AA treated cells. We next tested the effect of 9AA on cell cycle by fluorescence-activated cell sorting (FACS) analysis. HTLV-1-transformed C8166 and MT2 cells as well as control CEM cells were treated with 20 μM 9AA for 72 h. At the end of the incubation period, cells were harvested, stained with PI, and analyzed by FACS. The results presented in Fig. 2A demonstrate that treatment of C8166 or MT2 cells with 9AA leads to the appearance of a significant population of cells in the sub-G_1 peak. In C8166 cells, while DMSO control cells had only 1% of cells in sub-G_1, the 9AA-treated cells increased to about 43% at 72 h. Similarly, in MT2 cells, the number of cells in sub-G_1 increased to 33% (Fig. 2A). In contrast, the percentages of CEM cells and PBMCs in the sub-G_1 peak following 9AA treatment were significantly less (Fig. 2B and C).

To further quantify the level of apoptosis induced by 9AA, a BrdU-based TUNEL assay was performed. Consistent with the FACS analysis, when C8166 and MT2 cells were treated with 20 μM 9AA for 24 h, the number of TUNEL-positive cells in C8166 and MT2 cultures increased to 40 to 60%, compared to 5 to 8% TUNEL-positive cells in the DMSO-treated cells (Fig. 2C). Treatment of control CEM cells with 9AA showed significantly lower levels of apoptosis (5% or less). Our results suggest, therefore, that 9AA preferentially induces apoptosis in HTLV-1-transformed cells.

9AA-induced cell death is concentration and time dependent. To further compare the sensitivity of HTLV-1-transformed cells to 9AA, concentration- and time-dependent cell viability analysis of the 9AA-treated cells was performed. HTLV-1-transformed C8166, Hut102, and MT2 cells were treated with 5 to 20 μM 9AA for 24 to 48 h. At the end of the incubation period, cells were harvested, and cell viability was measured by a CellTiter-Glo luminescent cell viability kit (Promega). The results presented in Fig. 3A demonstrate a concentration-dependent increase in cell death. At the highest concentration of 9AA tested, 20 μM, approximately 90% of the C8166, Hut102, and MT2 cells were dead at 48 h posttreatment (Fig. 3A). The results presented in Fig. 3B demonstrate that the cell death observed following treatment of the cells with 20 μM 9AA was time dependent, with maximum cell death observed at 48 h. Overall, the Hut102 cells were slightly more sensitive to 9AA, followed by MT2 and C8166 cells.

Treatment of HTLV-1-transformed cells with 9AA increases p53 transcription activity. We next analyzed p53 protein and transcription activity in HTLV-1-transformed cells. The results presented in Fig. 4A demonstrate that even though there is a detectable level of p53 protein present in HTLV-1-transformed C8166 cells, there is a significant increase in p53 protein following treatment of the cells with increasing levels of 9AA. Elevated levels of p53 protein were observed at 9AA concentrations up to 20 μM and at later times of treatment including 24 and 48 h (Fig. 4A) (data not shown). While we did observed fluctuations in the levels of p53 protein induced from experiment to experiment following 9AA treatment, the levels

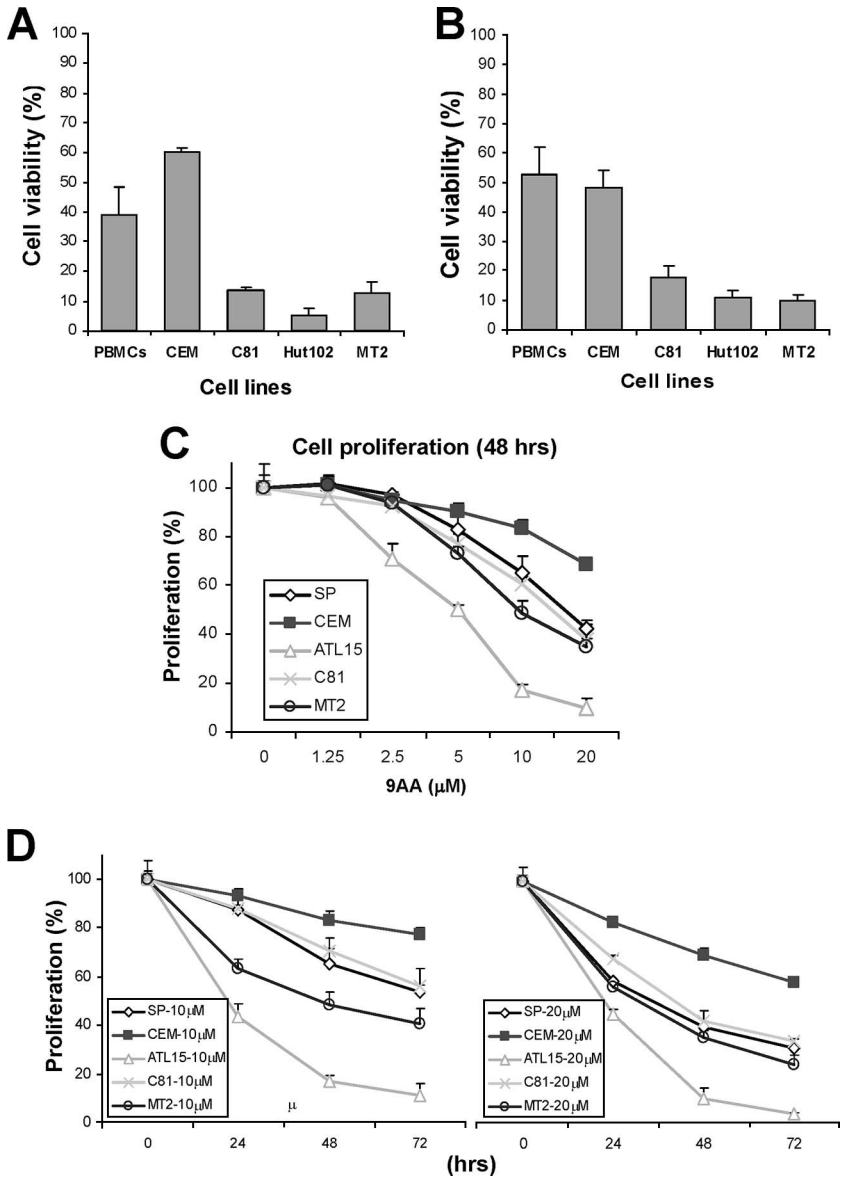

FIG. 1. 9AA induces cell death in HTLV-1-transformed cells. For the analysis of cell viability, a CellTiter-Glo luminescent cell viability assay (Promega) and trypan blue exclusion assay were used. (A and B) HTLV-1-transformed C8166 (C81), Hut102, and MT2 cells along with control PBMCs and CEM cells were treated with 20 μM 9AA for 48 h, and cell viability was measured by the CellTiter-Glo luminescent cell viability assay (A) or trypan blue exclusion assay (B). (C and D) HTLV-1-transformed C8166, MT2, and SP cells and ATL15 cells that are elutriated lymphocytes from an ATL patient, along with CEM cells, were treated with different doses of 9AA for 24 to 72 h (see Materials and Methods). Cell proliferation was measured by a nonradioactive cell proliferation assay. Values for 9AA-treated cells were compared to the signal for control vehicle DMSO-treated cells to determine percent cell viability. Values represent mean ± standard error with triplicate assays of four separate experiments.

were always significantly above the level detected in untreated cells. In parallel Western blots, we analyzed the expression of p53-responsive genes Mdm2 and p21. The results presented in Fig. 4A demonstrate that the expression of both Mdm2 and p21 was increased in C8166 cells following treatment with 9AA, consistent with an increase in p53 transcription activity. We also analyzed the level of p53, Mdm2, and p21 in the HTLV-1-transformed cell line MT2. As shown in Fig. 4A (right panel), similar to C8166 cells, MT2 cells showed increased levels of p53, Mdm2, and p21 following treatment with 9AA. We did note that while the level of Mdm2 induction was similar in C8166 and MT2 cells, the level of p21 induction was greater in the C8166 cells. The results presented in Fig. 4B demonstrated a time-dependent effect of 9AA on p53 protein and p53 transcription activity in C8166 cells.

Since Mdm2 is regulated at both the transcriptional and posttranscriptional levels, we performed RT-PCR to determine mRNA levels. The results presented in Fig. 4C demonstrate that there was an increase in Mdm2 but not control GAPDH transcription activity. By 48 h posttreatment, we observed approximately an 18-fold increase in Mdm2 mRNA.

Since Mdm2 and p21 promoter activity could be influenced

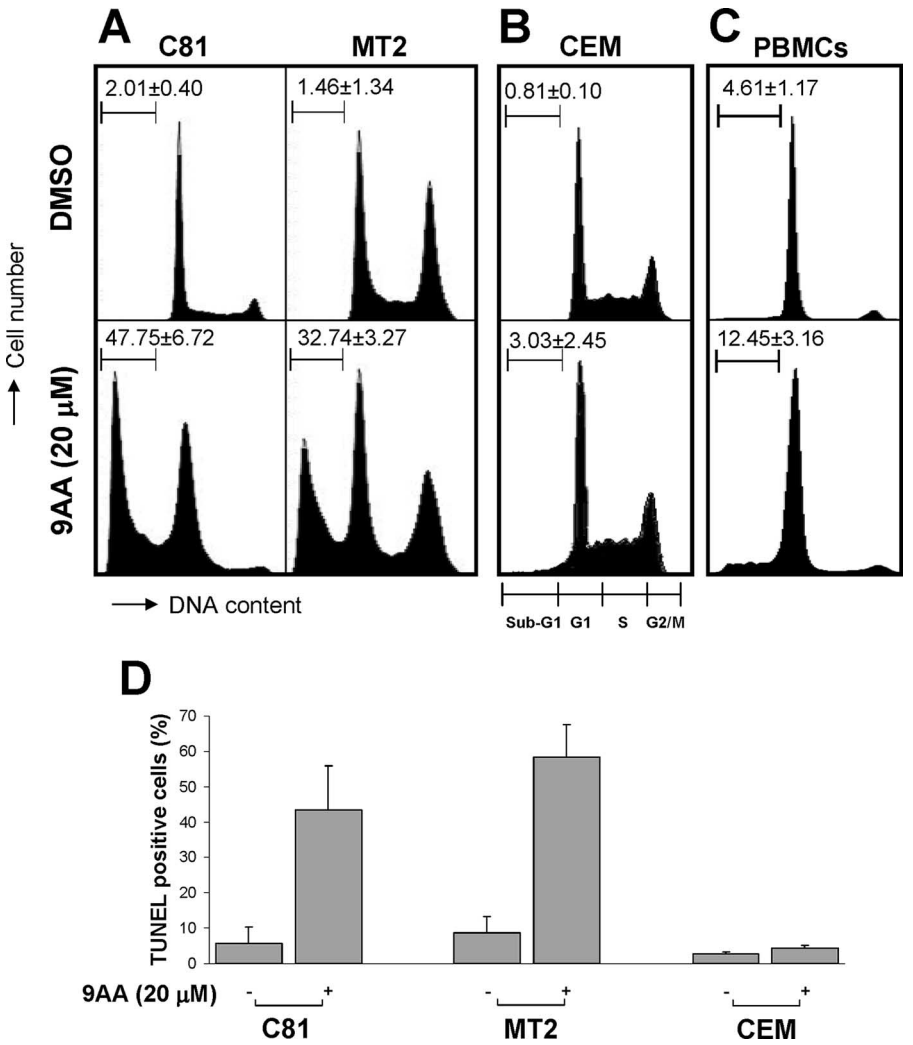

FIG. 2. 9AA induces apoptosis in HTLV-1-transformed cells. (A to C) HTLV-1-transformed C8166 (C81) cells and MT2 cells, HTLV-1-negative T-cell line CEM, or PBMCs were treated with 20 μM 9AA. At 72 h, cells were fixed with 70% ethanol, RNase treated, and stained with PI for flow cytometry analysis. Boundaries for sub-G_1, G_1, S, and G_2/M cell populations are presented under panel B. The percentage of cells in sub-G_1 and the boundaries are indicated in the upper-left-hand corner of each panel. (D) For TUNEL assay, C8166, MT2, and CEM cells were treated with 20 μM 9AA for 24 h. The cells were fixed with paraformaldehyde, followed by 70% ethanol. DNA breaks were labeled with TdT and BrdU triphosphate. Detection of BrdU triphosphate incorporation was through an Alexa-Fluor 488 dye-labeled anti-BrdU antibody analyzed by flow cytometry. Values represent means ± standard errors with triplicate assays of four separate experiments.

by transcription factors other than p53, we utilized the p53-responsive reporter plasmid PG13, which contains 13 consensus repeats of the p53 binding site upstream of the basal promoter to more directly measure p53 transcription activity. C8166 or control Jurkat cells were transfected with the PG13 reporter plasmid. Three hours posttransfection, cells were treated with 9AA or DMSO as a control. The results presented in Fig. 4D demonstrate that p53 transcription activity was dramatically increased in the presence of 9AA in C8166 cells. At 20 μM 9AA, a 12-fold increase in p53 transcription activity was observed. We found that the level of p53 transcription activity was increased, compared to control cells, up to 48 h after addition of 9AA (Fig. 4E). No increase of PG13 promoter activity was observed in control Jurkat cells, which do not have a functional p53 (Fig. 4D, panel 2), consistent with the hypothesis that this plasmid measures true p53 transcription activity.

Effect of 9AA on p65 and NF-κB activity in HTLV-1-transformed cells. We next analyzed the effect of 9AA on the NF-κB and upstream AKT and IκBα signaling pathways. The results shown in Fig. 5A demonstrate that 9AA decreases AKT phosphorylation and IκBα phosphorylation and protein level. Although the overall level of AKT remained fairly constant following treatment, phosphorylation at both AKT S473 and T308 was significantly reduced. We also noted that both the phosphorylation of IκBα and overall IκBα protein levels decreased following 9AA treatment. Interestingly, the level of phosphorylated AKT appears to increase slightly at 24 h. At present, the significance of this increase is unclear and will require further investigation.

We next analyzed the effect of 9AA on the level of nuclear accumulation of NF-κB subunits p50 and p65 and on NF-κB DNA binding and transcription activity. The results presented

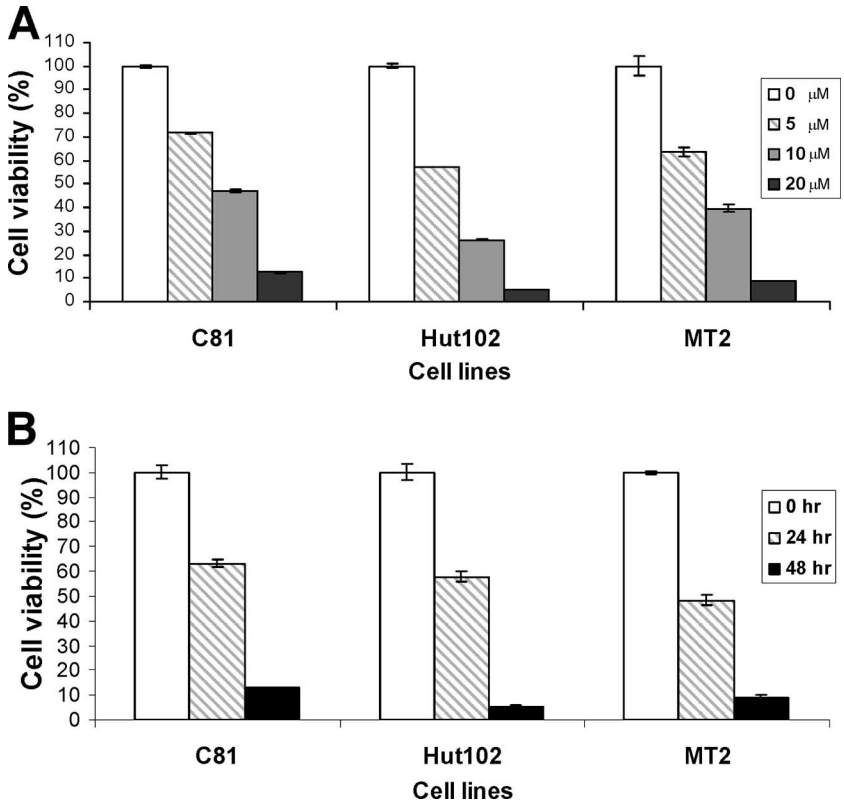

FIG. 3. 9AA-induced cell death in HTLV-1-transformed cells is concentration and time dependent. For the analysis of cell viability, a CellTiter-Glo luminescent cell viability kit (Promega) was used. (A) C8166 (C81), Hut102, and MT2 cells were treated with 5 to 20 μM 9AA for 48 h. At the end of the incubation period, cell viability was determined. (B) C8166, Hut102, and MT2 cells were treated with 20 μM 9AA for 24 or 48 h. At the end of the incubation period, cell viability was determined.

in Fig. 5A demonstrate several important points about the effect of 9AA. First, while the level of nuclear p50 did not change following treatment with 9AA (Fig. 5A, lower panels), we detected a significant increase in the level of nuclear p65. At the same time, however, there was a significant decrease in the level of phosphorylation of p65 at S536.

Given the change in p65 phosphorylation, we were interested in analyzing NF-κB binding and transcription activity. NF-κB binding activity was assayed using an EMSA. The results presented in Fig. 5B demonstrate a rather unexpected result that 9AA effectively decreases NF-κB DNA binding activity. At 20 μM 9AA, a 90% reduction in NF-κB binding activity was observed. The specificity of the gel shift complex was demonstrated by competition with wild type but not a mutant NF-κB oligonucleotide (Fig. 5B, lanes 2, 7, and 8). Consistent with the decrease in S536-phosphorylated p65 and NF-κB-DNA binding presented above (Fig. 5B) and with previous results by Gurova et al. (10), we observed that NF-κB promoter activity, as measured by 4X-NF-κB reporter activity, was significantly decreased in HTLV-1-transformed cells treated with 9AA (Fig. 5C).

Finally, we analyzed the expression of endogenous NF-κB-responsive cellular genes. Consistent with the above results, we found that the levels of NF-κB-responsive genes XIAP, cyclin D, and survivin were decreased following treatment with 9AA (Fig. 5D). In contrast, we did not see any decrease in expression from a control non-NF-κB-responsive gene such as tubulin (Fig. 5D).

9AA-induced apoptosis is p53 dependent in HTLV-1-transformed cells. Treatment of cells with 9AA induces activation of caspases linked to apoptosis. In view of the results of the FACS and TUNEL assays presented above, we were interested in determining which caspases were activated following treatment with 9AA. C8166 cells were treated with 20 μM 9AA for 24, 48, or 72 h. Cell extracts were then prepared and analyzed by Western blot analysis. The results presented in Fig. 6A demonstrate that 9AA induces the cleavage of caspase-9, caspase-3, and caspase-8. We also observed an increase in poly(ADP-ribose) polymerase (PARP) cleavage following 9AA treatment.

Lastly, we were interested in determining if 9AA inhibition of NF-κB and reactivation of p53 were linked to the cell death induced by 9AA. C8166 cells were infected with adeno-GFP or adeno-p53 siRNA. Forty-eight hours postinfection, 9AA was added to the culture medium as indicated, and cells were incubated for 48 h. As shown in Fig. 6B, infection of C8166 cells with adeno-p53 siRNA significantly reduced p53 expression in the absence or presence of 9AA (top panel, lanes 4 and 6). We next analyzed the effect of the p53 siRNA on p53 targets, PARP, and caspase-3. The results presented in Fig. 6B demonstrate that 9AA markedly increased PARP and caspase-3 cleavage in C8166 cells (panel 3, lanes 1 and 2). The siRNA-mediated silencing of p53 significantly reduced the

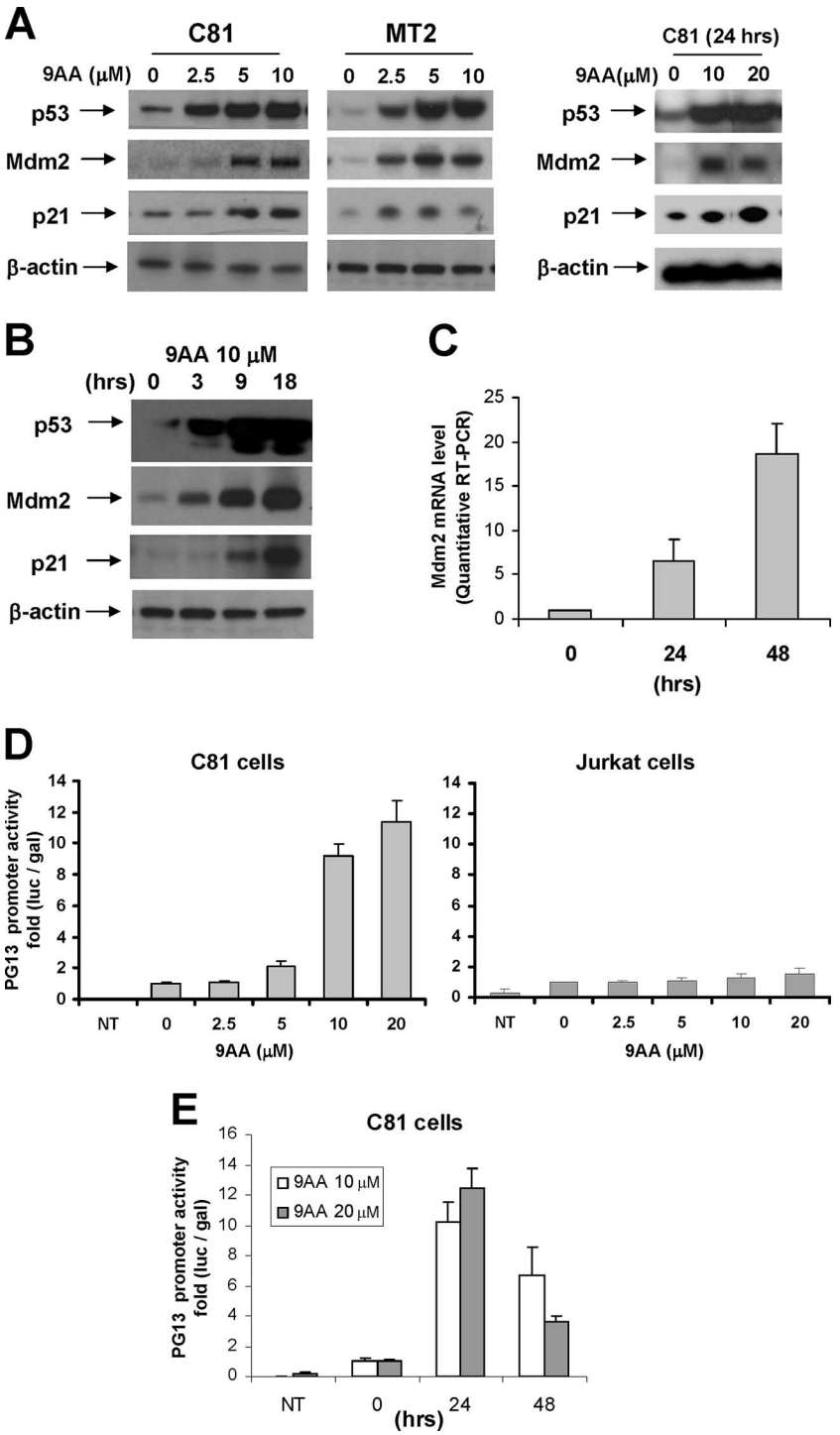

FIG. 4. 9AA reactivates p53 in HTLV-1-transformed cells. (A) C8166 (C81) and MT2 cells were treated with 9AA as indicated. Cells were incubated for 16 h posttreatment and harvested, and whole-cell was lysate prepared. p53, Mdm2, and p21 protein levels were checked by Western blotting. (B) C8166 cells were incubated with 10 μM 9AA. At indicated times of 0, 3, 9, and 18 h posttreatment, cells were harvested, and whole-cell extract was prepared. p53, Mdm2, and p21 proteins were analyzed by Western blotting. β-Actin was used as an internal loading control. (C) Quantitative RT-PCR was done to determine the *mdm2* mRNA level in total RNA from HTLV-1-transformed C8166 cells in the presence of 20 μM 9AA. The time of treatment with 9AA is indicated. (D) C8166 cells were transfected using the Transfast reagent with PG13-Luc (0.4 μg) and then cultured in the presence or absence of 9AA to measure endogenous p53 activity. Jurkat cells were used as a control for the absence of p53. (E) Transfected C8166 cells with PG13-Luc were treated with 9AA, and endogenous p53 activity was measured at different times. The results represent an average of at least four independent experiments. All luciferase values were adjusted for transfection efficiency using CMV β-galactosidase. Cells were harvested 24 h after transfection, and activity was measured. NT, not transfected; luc, luciferase; gal, galactosidase.

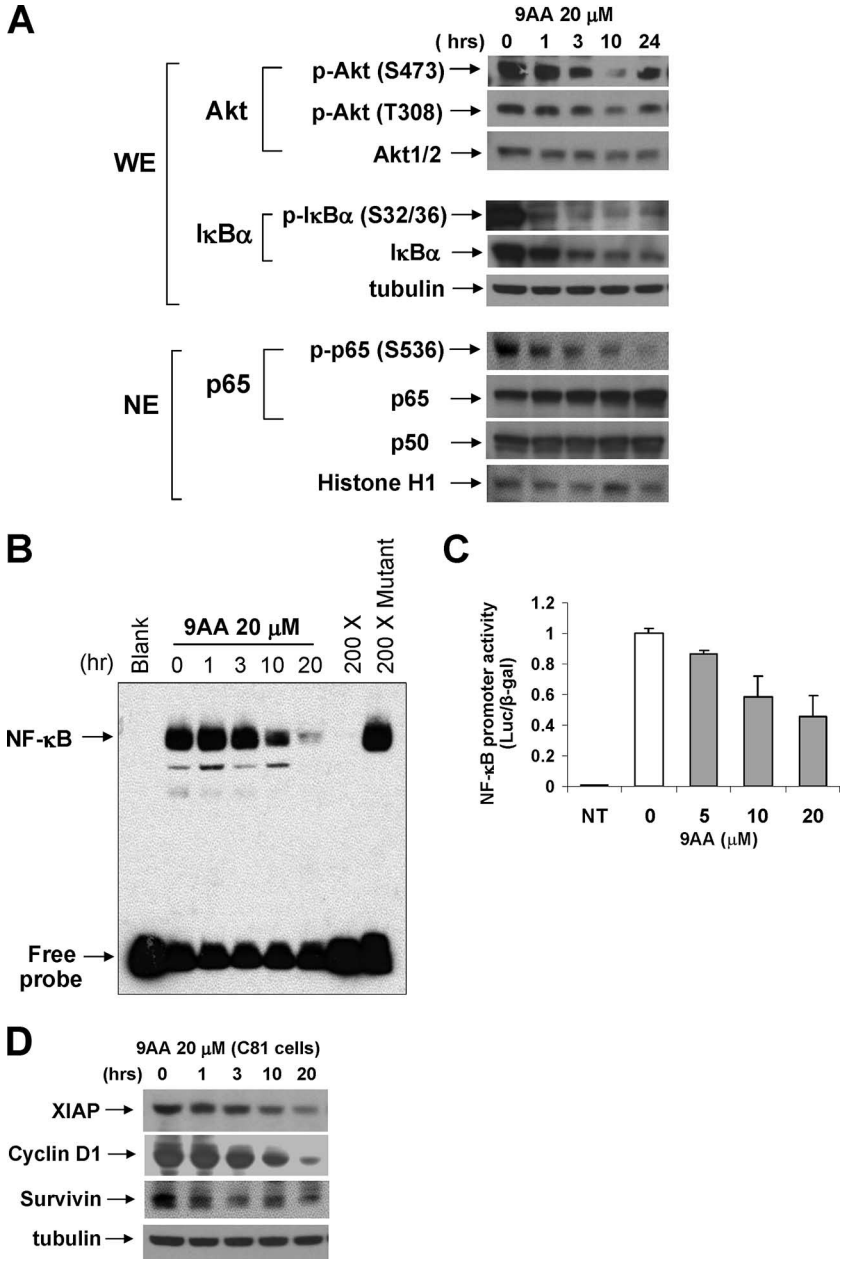

FIG. 5. 9AA inhibits NF-κB activation in HTLV-1 cells. (A) Whole-cell extract (WE; 100 μg) was immunoblotted with phospho-Akt or phospho-IκBα. Nuclear extract (NE; 100 μg) was immunoblotted with phospho-p65 (S536) antibodies, p65 or p50. β-Tubulin or histone H1 was used as a loading control. (B) Effect of 9AA on NF-κB DNA binding activity was assessed by EMSA using a consensus NF-κB oligonucleotide probe. C8166 cells were treated with 9AA, and nuclear extracts were prepared. For the competition assay, a 200 molar excess amount of unlabeled consensus or mutated consensus was used. (C) C8166 cells were transfected using Transfast reagent (Promega) with 5×NF-κB-Luc (0.5 μg). Three hours posttransfection, the cells were treated with 9AA (0, 5, and 10 μM). Cells were harvested 24 h later, and luciferase (Luc) activities were measured. The luciferase value was adjusted by CMV-β-galactosidase (β-gal) activity. Error bars represent the standard deviations of three independent experiments. (D) To examine cellular genes which are regulated by NF-κB, cell extracts from 9AA (20 μM)-treated C8166 (C81) cells were analyzed by Western blotting with anti-XIAP, anti-cyclin D, and anti-survivin antibodies. β-Tubulin was used as an internal loading control. NT, not treated.

9AA-induced PARP and caspase-3 cleavage (panels 3 and 4; compare lanes 4 and 6). Consistent with these results, we observed that the p53 siRNA significantly reduced 9AA-induced cell death as measured by the CellTiter-Glo luminescent cell viability assay. Cells treated with 10 μM 9AA and infected with the adeno-GFP virus exhibited approximately 40% cell death at 72 h (Fig. 6C). Remarkably, infection of the 9AA-treated cells with adeno-p53 siRNA resulted in less than 10% cell death at the same time point, a fourfold reduction in cell death. These results provide direct evidence that 9AA-induced cell death, at least in part, is due to the activity of p53 in the 9AA-treated cells.

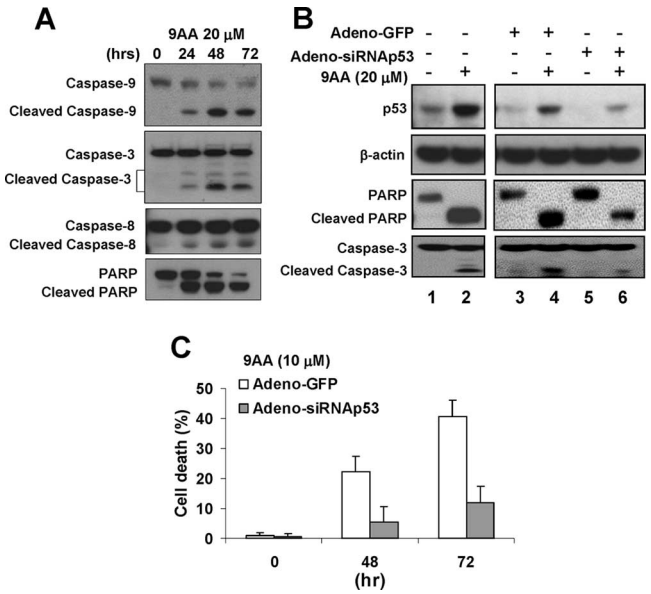

FIG. 6. 9AA induces p53-dependent apoptosis in C8166 cells. (A) C8166 cells were treated with 20 μM 9AA for 24 to 72 h; cells were harvested and lysed, and protein extract was used for detection of cleavage of caspase-9, caspase-3, caspase-8, and PARP by Western blotting. (B) C8166 cells were infected with adeno-GFP or adeno-p53 siRNA. At 48 h postinfection, the cells were treated with 20 μM 9AA. After incubation for 48 h, cells were harvested and extracted with cell lysis buffer, and protein extract was used for Western blotting with p53, PARP, caspase-3, and β-tubulin antibodies. (C) At 48 h postinfection, cells were treated with 10 μM 9AA for 48 to 72 h in a time-dependent manner, and cell viability was measured by the CellTiter-Glo luminescent cell viability assay (Promega). Values represent means ± standard errors with triplicate assays of four separate experiments.

DISCUSSION

The ability of p53 to respond to stress signals, triggering cell-cycle arrest and cell death by apoptosis, is crucial for the prevention of tumor development. Inactivation of p53 function by mutation, chromosomal deletion, or protein inhibition occurs in more than half of all human tumors (45). In HTLV-1-infected cells, Tax inhibits wild-type p53 transactivation function through a unique pathway involving p53 phosphorylation and activation of a unique NF-κB activation cascade (18, 34). In the present paper, we highlight the action of a drug that can inhibit NF-κB and reactivate p53 in HTLV-1-transformed cells.

9AA was initially identified as an antibacterial agent (42, 47). Subsequently, it was found that staining of histopathological sections with 9AA could be used to locate malignant cells in many tumor tissues. The positive staining was the result of the interaction between 9AA with guanidinobenzoatases (43). Most recently, 9AA has been utilized as an anticancer drug that targets two important stress-responsive pathways, NF-κB and p53, in RCC (10). Specifically, 9AA caused p53-dependent induction of apoptosis and growth arrest in RCC (10). In contrast to other DNA-damaging drugs, 9AA did not induce the phosphorylation of p53 except at amino acid S392. These observations suggested that 9AA uses a distinctive mechanism to activate p53 in the RCC cell line. During review of this article, it was demonstrated that 9AA reactivates p53 in human immunodeficiency virus (HIV)-infected cells (48). The authors demonstrate that, similar to our hypothesis, 9AA activates p53 in HIV type 1 (HIV-1)-infected lymphocytes and may be a target for therapeutic attack.

Earlier studies from this laboratory have shown that p53 in most HTLV-1 cells is wild type in sequence but is functionally inhibited by the HTLV-1 Tax protein through induction of a novel NF-κB pathway (18, 34). The ability to simultaneously inhibit NF-κB and activate p53 has several potential advantages in anticancer therapy. NF-κB activation is normally a pro cell growth signal, activating several proliferation pathways while at the same time inhibiting apoptosis. The constitutive activation of NF-κB in tumor cells, therefore, aids in the uncontrolled proliferation of these cells and contributes to the lack of response to apoptotic signals. Inhibiting NF-κB would decrease proliferation as well as make the tumor cells responsive to apoptosis signals. Activation of relatively abundant levels of transcriptionally inactive p53 in the tumor cells, on the other hand, would provide a selective mechanism to detect cell stress signals and induce cell death. Along these lines Datta et al. (6) have shown that ATL patients carrying a wild-type p53 enter remission following treatment with AZT while those with a mutated p53 did not respond (5). Moreover, the patients' disease relapse was associated with the selection of a tumor clone carrying mutated inactive p53.

In this study, we provide evidence that 9AA effectively and preferentially induced apoptosis in HTLV-1-transformed cells. 9AA treatment results in the dramatic increase in the level of p53 protein, which is accompanied by an increase in p53 transcription activity. We show this both by analysis of endogenous cellular genes as well as activation of a p53-responsive reporter plasmid. Most importantly, a p53 siRNA dramatically reduced apoptotic cell death in 9AA-treated cells. This result provides direct evidence that links the p53 reactivation and apoptosis pathways.

NF-κB activation is triggered by activation of the upstream IKK complex by kinases that include AKT. Activated IKK phosphorylates IκBα, which results in ubiquitination and proteosomal degradation of the inhibitory subunit. Degradation of IκBα releases active p50/p65 heterodimers, which are translocated to the nucleus to activate transcription. 9AA treatment of the HTLV-1-transformed cells showed significant decreases in AKT signaling, IκB phosphorylation, and NF-κB activity.

Although 9AA inhibits NF-κB and activates p53 in both RCC and HTLV-1-transformed cells, it is clear that there may be differences in the mode of action in the two cell types. First, in RCC cells there was a dramatic effect of 9AA on protein accumulation, with a general inhibition of translation in RCC cells. In contrast, in HTLV-1-transformed C8166 cells, an increase in proteins such as p53 and p53-responsive proteins p21 and Mdm2 at 9AA concentrations up to 20 μM was observed. Second, while we observed a decrease in AKT phosphorylation at both S473 and T308, in RCC cells S473 but not T308 phosphorylation was decreased (K. Gurova, unpublished data). Third, in RCC cells, the distinct decrease in IκBα phosphorylation was not observed. Lastly, a decrease in NF-κB DNA binding in EMSAs was observed in the HTLV-1-transformed C8166 cells. In contrast, 9AA treatment of RCC cells led to an increase in binding of an inactive NF-κB complex. While there were differences in the NF-κB DNA binding activity response,

NF-κB transcription activity was decreased in both HTLV-1 and RCC cells. In the more recent study by Wu et al., a clear mechanism of action of 9AA in HIV-1-infected cells was not determined; however, it was suggested to involve p53 S15 phosphorylation and disruption of the Tat-p53 complex (48).

In previous studies, we have analyzed the ability of small-molecule inhibitors LY294002 and SC514 to inhibit NF-κB and activate p53 in HTLV-1-transformed cells. While both of these compounds were able to inhibit NF-κB, resulting in reactivation of p53, both compounds were significantly weaker than 9AA in p53 reactivation. Thus, while the molecular mechanism remains to be determined, the results suggest that 9AA effectively targets key components of the p53 inhibition pathway. The fact that 9AA induced apoptosis in HTLV-1-transformed cells but not control T lymphocytes and PBMCs suggests that the drug has potential to selectively target tumor cells.

REFERENCES

1. **Akagi, T., H. Ono, and K. Shimotohno.** 1995. Characterization of T cells immortalized by Tax1 of human T-cell leukemia virus type 1. Blood **86:**4243–4249.
2. **Asquith, B., A. J. Mosley, A. Heaps, Y. Tanaka, G. P. Taylor, A. R. McLean, and C. R. Bangham.** 2005. Quantification of the virus-host interaction in human T lymphotropic virus I infection. Retrovirology **2:**75.
3. **Bangham, C. R., and M. Osame.** 2005. Cellular immune response to HTLV-1. Oncogene **24:**6035–6046.
4. **Bex, F., and R. B. Gaynor.** 1998. Regulation of gene expression by HTLV-I Tax protein. Methods **16:**83–94.
5. **Datta, A., M. Bellon, U. Sinha-Datta, A. Bazarbachi, Y. Lepelletier, D. Canioni, T. A. Waldmann, O. Hermine, and C. Nicot.** 2006. Persistent inhibition of telomerase reprograms adult T-cell leukemia to p53-dependent senescence. Blood **108:**1021–1029.
6. **Datta, S. R., A. Brunet, and M. E. Greenberg.** 1999. Cellular survival: a play in three Akts. Genes Dev. **13:**2905–2927.
7. **de La Fuente, C., L. Deng, F. Santiago, L. Arce, L. Wang, and F. Kashanchi.** 2000. Gene expression array of HTLV type 1-infected T cells: up-regulation of transcription factors and cell cycle genes. AIDS Res. Hum. Retrovir. **16:**1695–1700.
8. **Grassmann, R., C. Dengler, I. Muller-Fleckenstein, B. Fleckenstein, K. McGuire, M. C. Dokhelar, J. G. Sodroski, and W. A. Haseltine.** 1989. Transformation to continuous growth of primary human T lymphocytes by human T-cell leukemia virus type I X-region genes transduced by a herpesvirus Saimiri vector. Proc. Natl. Acad. Sci. USA **86:**3351–3355.
9. **Grossman, W. J., J. T. Kimata, F. H. Wong, M. Zutter, T. J. Ley, and L. Ratner.** 1995. Development of leukemia in mice transgenic for the tax gene of human T-cell leukemia virus type I. Proc. Natl. Acad. Sci. USA **92:**1057–1061.
10. **Gurova, K. V., J. E. Hill, C. Guo, A. Prokvolit, L. G. Burdelya, E. Samoylova, A. V. Khodyakova, R. Ganapathi, M. Ganapathi, N. D. Tararova, D. Bosykh, D. Lvovskiy, T. R. Webb, G. R. Stark, and A. V. Gudkov.** 2005. Small molecules that reactivate p53 in renal cell carcinoma reveal a NF-κB-dependent mechanism of p53 suppression in tumors. Proc. Natl. Acad. Sci. USA **102:**17448–17453.
11. **Hasegawa, H., H. Sawa, M. J. Lewis, Y. Orba, N. Sheehy, Y. Yamamoto, T. Ichinohe, Y. Tsunetsugu-Yokota, H. Katano, H. Takahashi, J. Matsuda, T. Sata, T. Kurata, K. Nagashima, and W. W. Hall.** 2006. Thymus-derived leukemia-lymphoma in mice transgenic for the Tax gene of human T-lymphotropic virus type I. Nat. Med. **12:**466–472.
12. **Hinrichs, S. H., M. Nerenberg, R. K. Reynolds, G. Khoury, and G. Jay.** 1987. A transgenic mouse model for human neurofibromatosis. Science **237:**1340–1343.
13. **Hiscott, J., H. Kwon, and P. Genin.** 2001. Hostile takeovers: viral appropriation of the NF-κB pathway. J. Clin. Investig. **107:**143–151.
14. **Jeang, K. T.** 2001. Functional activities of the human T-cell leukemia virus type I Tax oncoprotein: cellular signaling through NF-κB. Cytokine Growth Factor Rev. **12:**207–217.
15. **Jeang, K. T., C. Z. Giam, F. Majone, and M. Aboud.** 2004. Life, death, and tax: role of HTLV-I oncoprotein in genetic instability and cellular transformation. J. Biol. Chem. **279:**31991–31994.
16. **Jeong, S. J., A. Dasgupta, K. J. Jung, J. H. Um, A. Burke, H. U. Park, and J. N. Brady.** 2008. PI3K/AKT inhibition induces caspase-dependent apoptosis in HTLV-1-transformed cells. Virology **370:**264–272.
17. **Jeong, S. J., C. A. Pise-Masison, M. F. Radonovich, H. U. Park, and J. N. Brady.** 2005. Activated AKT regulates NF-κB activation, p53 inhibition and cell survival in HTLV-1-transformed cells. Oncogene **24:**6719–6728.
18. **Jeong, S. J., M. Radonovich, J. N. Brady, and C. A. Pise-Masison.** 2004. HTLV-I Tax induces a novel interaction between p65/RelA and p53 that results in inhibition of p53 transcriptional activity. Blood **104:**1490–1497.
19. **Jiang, X., N. Takahashi, N. Matsui, T. Tetsuka, and T. Okamoto.** 2003. The NF-κB activation in lymphotoxin beta receptor signaling depends on the phosphorylation of p65 at serine 536. J. Biol. Chem. **278:**919–926.
20. **Kehn, K., R. Berro, C. de la Fuente, K. Strouss, E. Ghedin, S. Dadgar, M. E. Bottazzi, A. Pumfery, and F. Kashanchi.** 2004. Mechanisms of HTLV-1 transformation. Front Biosci. **9:**2347–2372.
21. **Kerkhofs, P., H. Heremans, A. Burny, R. Kettmann, and L. Willems.** 1998. In vitro and in vivo oncogenic potential of bovine leukemia virus G4 protein. J. Virol. **72:**2554–2559.
22. **Kim, S. J., T. S. Winokur, H. D. Lee, D. Danielpour, K. Y. Kim, A. G. Geiser, L. S. Chen, M. B. Sporn, A. B. Roberts, and G. Jay.** 1991. Overexpression of transforming growth factor-beta in transgenic mice carrying the human T-cell lymphotropic virus type I tax gene. Mol. Cell. Biol. **11:**5222–5228.
23. **Madrid, L. V., M. W. Mayo, J. Y. Reuther, and A. S. Baldwin, Jr.** 2001. Akt stimulates the transactivation potential of the RelA/p65 subunit of NF-κB through utilization of the IκB kinase and activation of the mitogen-activated protein kinase p38. J. Biol. Chem. **276:**18934–18940.
24. **Mayo, L. D., and D. B. Donner.** 2002. The PTEN, Mdm2, p53 tumor suppressor-oncoprotein network. Trends Biochem. Sci. **27:**462–467.
25. **Nerenberg, M., S. H. Hinrichs, R. K. Reynolds, G. Khoury, and G. Jay.** 1987. The *tat* gene of human T-lymphotropic virus type 1 induces mesenchymal tumors in transgenic mice. Science **237:**1324–1329.
26. **Okamoto, T., Y. Ohno, S. Tsugane, S. Watanabe, M. Shimoyama, K. Tajima, M. Miwa, and K. Shimotohno.** 1989. Multi-step carcinogenesis model for adult T-cell leukemia. Jpn. J. Cancer Res. **80:**191–195.
27. **O'Mahony, A. M., M. Montano, K. Van Beneden, L. F. Chen, and W. C. Greene.** 2004. Human T-cell lymphotropic virus type 1 tax induction of biologically Active NF-κB requires IκB kinase-1-mediated phosphorylation of RelA/p65. J. Biol. Chem. **279:**18137–18145.
28. **Orlowski, R. Z., and A. S. Baldwin, Jr.** 2002. NF-κB as a therapeutic target in cancer. Trends Mol. Med. **8:**385–389.
29. **Oya, M., A. Takayanagi, A. Horiguchi, R. Mizuno, M. Ohtsubo, K. Marumo, N. Shimizu, and M. Murai.** 2003. Increased nuclear factor-kappa B activation is related to the tumor development of renal cell carcinoma. Carcinogenesis **24:**377–384.
30. **Ozes, O. N., L. D. Mayo, J. A. Gustin, S. R. Pfeffer, L. M. Pfeffer, and D. B. Donner.** 1999. NF-κB activation by tumour necrosis factor requires the Akt serine-threonine kinase. Nature **401:**82–85.
31. **Peloponese, J. M., Jr., and K. T. Jeang.** 2006. Role for Akt/protein kinase B and activator protein-1 in cellular proliferation induced by the human T-cell leukemia virus type 1 tax oncoprotein. J. Biol. Chem. **281:**8927–8938.
32. **Pise-Masison, C. A., and J. N. Brady.** 2005. Setting the stage for transformation: HTLV-1 Tax inhibition of p53 function. Front. Biosci. **10:**919–930.
33. **Pise-Masison, C. A., S. J. Jeong, and J. N. Brady.** 2005. Human T cell leukemia virus type 1: the role of Tax in leukemogenesis. Arch. Immunol. Ther. Exp. **53:**283–296.
34. **Pise-Masison, C. A., R. Mahieux, H. Jiang, M. Ashcroft, M. Radonovich, J. Duvall, C. Guillerm, and J. N. Brady.** 2000. Inactivation of p53 by human T-cell lymphotropic virus type 1 Tax requires activation of the NF-κB pathway and is dependent on p53 phosphorylation. Mol. Cell. Biol. **20:**3377–3386.
35. **Pise-Masison, C. A., R. Mahieux, M. Radonovich, H. Jiang, and J. N. Brady.** 2001. Human T-lymphotropic virus type I Tax protein utilizes distinct pathways for p53 inhibition that are cell type-dependent. J. Biol. Chem. **276:**200–205.
36. **Pozzatti, R., J. Vogel, and G. Jay.** 1990. The human T-lymphotropic virus type I tax gene can cooperate with the *ras* oncogene to induce neoplastic transformation of cells. Mol. Cell. Biol. **10:**413–417.
37. **Prives, C., and P. A. Hall.** 1999. The p53 pathway. J. Pathol. **187:**112–126.
38. **Ratner, L., T. Portis, M. Robek, J. Harding, and W. Grossman.** 2000. Studies of the immortalizing activity of HTLV type 1 Tax, using an infectious molecular clone and transgenic mice. AIDS Res. Hum Retrovir. **16:**1647–1651.
39. **Romashkova, J. A., and S. S. Makarov.** 1999. NF-κB is a target of AKT in anti-apoptotic PDGF signalling. Nature **401:**86–90.
40. **Sakurai, H., H. Chiba, H. Miyoshi, T. Sugita, and W. Toriumi.** 1999. IκB kinases phosphorylate NF-κB p65 subunit on serine 536 in the transactivation domain. J. Biol. Chem. **274:**30353–30356.
41. **Sizemore, N., S. Leung, and G. R. Stark.** 1999. Activation of phosphatidylinositol 3-kinase in response to interleukin-1 leads to phosphorylation and activation of the NF-κB p65/RelA subunit. Mol. Cell. Biol. **19:**4798–4805.
42. **Stark, M. M., N. C. Hall, R. J. Nicholson, and K. Soelberg.** 1968. 9-Aminoacridine, an effective antibacterial agent with caries-disclosing features. Oral. Surg. Oral. Med. Oral Pathol. **26:**560–562.
43. **Steven, F. S., U. Suresh, T. L. Wong, and M. M. Griffin.** 1987. The role of

inhibitors in the fluorescent staining of benign naevus and malignant melanoma cells with 9-amino acridine and acridine orange. J. Enzyme Inhib. **1:**275–287.
44. **Tanaka, A., C. Takahashi, S. Yamaoka, T. Nosaka, M. Maki, and M. Hatanaka.** 1990. Oncogenic transformation by the tax gene of human T-cell leukemia virus type I in vitro. Proc. Natl. Acad. Sci. USA **87:**1071–1075.
45. **Vogelstein, B., D. Lane, and A. J. Levine.** 2000. Surfing the p53 network. Nature **408:**307–310.
46. **Vousden, K. H., and X. Lu.** 2002. Live or let die: the cell's response to p53. Nat. Rev. Cancer **2:**594–604.
47. **Wainwright, M.** 2001. Acridine-a neglected antibacterial chromophore. J. Antimicrob. Chemother. **47:**1–13.
48. **Wu, W., K. Kehn-Hall, C. Pedati, L. Zweier, I. Castro, Z. Klase, C. S. Dowd, L. Dubrovsky, M. Bukrinsky, and F. Kashanchi.** 2008. Drug 9AA reactivates p21/Waf1 and Inhibits HIV-1 progeny formation. Virol. J. **5:**41.
49. **Yoshida, M.** 2001. Multiple viral strategies of HTLV-1 for dysregulation of cell growth control. Annu. Rev. Immunol. **19:**475–496.